An Important Role for *N*-Acylethanolamine Acid Amidase in the Complete Freund's Adjuvant Rat Model of Arthritis[S]

F. T. Bonezzi, O. Sasso, S. Pontis, N. Realini, E. Romeo, S. Ponzano, A. Nuzzi, A. Fiasella, F. Bertozzi, and D. Piomelli

Drug Discovery and Development, Istituto Italiano di Tecnologia, Genova, Italy (F.T.B., O.S., S.P., N.R., E.R., S.P., A.N., A.F., F.B., D.P.); and Departments of Anatomy and Neurobiology, Pharmacology and Biological Chemistry, University of California, Irvine, California (D.P.)

ABSTRACT

The endogenous lipid amides, palmitoylethanolamide (PEA) and oleoylethanolamide (OEA), exert marked antinociceptive and anti-inflammatory effects in animal models by engaging nuclear peroxisome proliferator-activated receptor-α. PEA and OEA are produced by macrophages and other host-defense cells and are deactivated by the cysteine amidase, *N*-acylethanolamine acid amidase (NAAA), which is highly expressed in macrophages and B-lymphocytes. In the present study, we examined whether a) NAAA might be involved in the inflammatory reaction triggered by injection of complete Freund's adjuvant (CFA) into the rat paw and b) administration of 4-cyclohexylbutyl-*N*-[(S)-2-oxoazetidin-3-yl]-carbamate (ARN726), a novel systemically active NAAA inhibitor, attenuates such reaction. Injection of CFA into the paw produced local edema and heat hyperalgesia, which were accompanied by decreased PEA and OEA content (assessed by liquid chromatography/mass spectrometry) and increased NAAA levels (assessed by Western blot and ex vivo enzyme activity measurements) in paw tissue. Administration of undec-10-ynyl-*N*-[(3S)-2-oxoazetidin-3-yl] carbamate (ARN14686), a NAAA-preferring activity-based probe, revealed that NAAA was catalytically active in CFA-treated paws. Administration of ARN726 reduced NAAA activity and restored PEA and OEA levels in inflamed tissues, and significantly decreased CFA-induced inflammatory symptoms, including pus production and myeloperoxidase activity. The results confirm the usefulness of ARN726 as a probe to investigate the functions of NAAA in health and disease and suggest that this enzyme may provide a new molecular target for the treatment of arthritis.

Introduction

Macrophages and other cellular components of the body's host-defense system produce a variety of lipid-derived mediators that are involved in the promotion of inflammation. For example, they are a major source of eicosanoids, local signals that recruit blood-borne immune cells to injury sites and cause vasodilation and nociceptor sensitization (Laskin et al., 2011). An expanding body of evidence suggests, however, that host-defense cells can also produce biologically active lipids that attenuate, rather than enhance, pain and inflammation. This group of lipids includes palmitoylethanolamide (PEA) and oleoylethanolamide (OEA), two long-chain fatty acid ethanolamides (FAE) that exert marked anti-inflammatory effects by activating the nuclear receptor peroxisome proliferator-activated receptor-α (PPAR-α) (Fu et al., 2003; LoVerme et al., 2005; Piomelli and Sasso, 2014).

In macrophages, the modulatory actions of PEA and OEA on the inflammatory process are stopped by the intracellular hydrolysis of these substances, which is catalyzed by the cysteine amidase *N*-acylethanolamine acid amidase (NAAA) (Tsuboi et al., 2005; Ribeiro et al., 2015). The cellular localization of this enzyme—which is highly concentrated in macrophages and B-lymphocytes compared with other cell lineages (Tsuboi et al., 2005; Ribeiro et al., 2015)—is suggestive of a role in the regulation of innate immune responses. A small number of pharmacological studies support this idea. For example, recent experiments have shown that the compound 4-cyclohexylbutyl-*N*-[(S)-2-oxoazetidin-3-yl]-carbamate) (ARN726)—a systemically active β-lactam-based NAAA inhibitor—suppresses both lung inflammation in mice, via a mechanism that requires PPAR-α activation, and endotoxin-induced responses in human macrophages (Ribeiro et al., 2015). These results suggest that NAAA inhibition might offer a novel mechanistic approach to treat human inflammatory conditions, such as rheumatoid arthritis and osteoarthritis, in which the levels of PEA and OEA are markedly reduced (Richardson et al., 2008).

As a direct test of this idea, in the present study we examined whether NAAA might be involved in the inflammatory reaction elicited by complete Freund's adjuvant (CFA) in

ABBREVIATIONS: ARN14686, undec-10-ynyl-*N*-[(3S)-2-oxoazetidin-3-yl] carbamate; ARN726, 4-cyclohexylbutyl-*N*-[(S)-2-oxoazetidin-3-yl]-carbamate; CFA, complete Freund's adjuvant; DRG, dorsal root ganglia; FAE, fatty acid ethanolamide; H&E, hematoxylin and eosin; LPS, lipopolysaccharide; MPO, myeloperoxidase; NAAA, *N*-acylethanolamine acid amidase; OEA, oleoylethanolamide; PBS, phosphate-buffered saline; PE, phosphatidylethanolamine; PEA, palmitoylethanolamide; PPAR-α, peroxisome proliferator-activated receptor-α; (S)-OOPP, *N*-[(3S)-2-oxo-3-oxetanyl]-3-phenylpropanamide; TBS, Tris-buffered saline.

rats, and whether systemic administration of ARN726 attenuates such reaction. We found that CFA-induced paw inflammation is accompanied by a substantial increase in NAAA levels, and a concomitant decrease in local PEA and OEA content. Using the NAAA-selective activity-based probe, undec-10-ynyl-N-[(3S)-2-oxoazetidin-3-yl] carbamate (ARN14686) (Romeo et al., 2015), we demonstrate that the enzyme that accumulates in CFA-treated paws is catalytically active. Finally, we show that administration of ARN726 substantially decreases CFA-induced inflammatory symptoms, including edema, heat hyperalgesia, pus production, and myeloperoxidase activity. The results implicate NAAA in the genesis of CFA-induced inflammation and suggest a potential application for NAAA inhibitors in the treatment of arthritis.

Materials and Methods

Animals. Male Sprague-Dawley rats weighing 280–300 g were purchased from Charles River (Lecco, Italy) and housed in groups of three in ventilated cages lined with autoclaved cellulose paper with free access to food and water. They were maintained under a 12-hour light/dark cycle (lights on at 8:00 AM), at controlled temperature (21 ± 1°C) and relative humidity (55 ± 10%). All procedures were in accordance with the Ethical Guidelines of the International Association for the Study of Pain, with Italian regulations on protection of animals used for experimental and other scientific purposes (D.M. 116192) as well as with European Union regulations (O.J. of E.C. L 358/1 12/18/1986).

Chemicals. ARN726 was synthesized as described (Ribeiro et al., 2015). Dexamethasone was purchased from Sigma-Aldrich (St. Louis, MO). Drug solutions were prepared immediately before use in a vehicle consisting of 80% saline, 10% PEG 400, and 10% Tween 80. The following doses were used: ARN726: 3, 10, and 30 mg/kg i.p. administration; dexamethasone: 10 mg/kg oral administration.

Experimental Design. CFA (Sigma-Aldrich, 150 μl, 1 mg/ml) was injected into the left hindpaw of rats anesthetized with 2–3% isoflurane. Behavioral tests were performed before injection and 7 and 14 days later, as previously described (Sasso et al., 2012). Drug treatments were carried out 7 and 14 days after CFA injection; behavioral assays were conducted 1 and 4 hours after the treatments. Rats were randomly divided into groups of 10 for each treatment. Behavioral testing was performed between 9:00 AM and 5:00 PM under blinded conditions (investigators conducting the measurements were unaware of treatment). Furthermore, two groups of animals were treated with vehicle given intraperitoneally or orally.

Behavioral Assays. Paw volume was measured in both ipsilateral (injected) and contralateral (noninjected) paws using a plethysmometer (Ugo Basile, Comerio, Italy) (Sasso et al., 2012). Thermal hyperalgesia was assessed as described (Hargreaves et al., 1988), measuring the latency to withdraw hindpaws from a focused beam of radiant heat (thermal intensity: infrared 5.0) in a plantar test apparatus (Ugo Basile). Cut-off time was set at 30 seconds. Withdrawal latencies were measured three times. Rats were fully awake at every time point.

Tissue Collection. Paws and dorsal root ganglia (DRG, L4-L5-L6) from ipsilateral and contralateral sides of control and CFA-injected rats were collected 7 and 14 days after CFA injection. Rats were killed, and tissues were immediately frozen in liquid nitrogen and stored at −80°C.

Lysosomal Enrichment. Paws were dissected, skin and bones were removed, and the remaining tissue was homogenized with a Polytron homogenizer in 1:9 (v/w) of ice-cold 20 mM Tris-HCl (pH 7.4) containing 0.32 M sucrose, then centrifuged at 800 g for 15 minutes (4°C). DRG (L4-L5-L6) tissue was subjected to a similar treatment. Supernatants were collected and centrifuged at 12,000 g for 30 minutes

(4°C). Pellets were weighed, suspended in phosphate-buffered saline (PBS; 2 ml for 1 g of pellet), placed at −80°C for 1 hour, thawed at room temperature, and then stored at −80°C overnight. The following day, samples were thawed at room temperature and centrifuged at 105,000 g for 1 hour (4°C), and the soluble fraction was collected. Protein concentration was measured by bicinchoninic acid colorimetric protein assay (Thermo Scientific, Milan, Italy).

NAAA Activity Assay. Lysosomal-enriched samples (20 μg of enriched obtained as described above) were incubated in assay buffer (pH 4.5; 150 mM NaCl, 100 mM trisodium citrate dihydrate, 100 mM sodium phosphate monobasic, NaH_2PO_4, 0,1% Nonidet P-40, and 3 mM dithiothreitol) in a total volume of 190 μl. NAAA substrate (heptadecanoyl-ethanolamide, 50 μM) was added, and the mixture was incubated at 37°C in a water bath for 2 hours (paw samples) or 4 hours (DRG samples). Reactions were stopped with 600 μl of stop solution (cold chloroform: methanol; 2:1 v/v) containing 1 nmol heptadecanoic acid (NuChek Prep Waterville, MN) as internal standard. Samples were centrifuged at 2095 g for 15 minutes (4°C); organic phases were collected, dried under nitrogen, and resuspended in 75 μl of methanol. Samples (injection volume = 5 μl) were eluted isocratically on an Acquity UPLC BEH C18 column (50 mm length, 2.1 mm i.d., 1.7 μm pore size, Waters, Milford, MA) at 0.5 ml/min for 1.5 minutes with a solvent mixture of 95% methanol and 5% water, both containing 0.25% acetic acid and 5 mM ammonium acetate. Column temperature was set at 40°C. Electrospray ionization was in the negative mode, capillary voltage was 2.7 kV, cone voltage was 45 kV, and source temperature was 150°C with a desolvation temperature of 450°C. Nitrogen was used as drying gas at a flow rate of 800 l/h and a temperature of 500°C. The $[M-H]^-$ ion was monitored in the selected-ion monitoring mode (m/z values: heptadecenoic acid 267.37, heptadecanoic acid, 269.37). Calibration curves were generated using authentic heptadecenoic acid.

Western Blot Analyses. Lysosomal-enriched samples (20 μg of enriched samples) were denatured in 8% sodium dodecyl sulfate (SDS) and 5% β-mercaptoethanol at 99°C for 3 minutes. After separation by SDS-PAGE on a 4–15% gel (Bio-Rad, Hercules, CA) under denaturing conditions, proteins were electrotransferred to nitrocellulose membranes. Membranes were blocked with 5% non-fat dry milk in Tris-buffered saline (TBS) and then incubated overnight with anti-NAAA antibody (1:1,000; R&D Systems, Minneapolis, MN) and anti-alpha tubulin antibody (1:2000; Abcam, Cambridge, UK) in 1% non-fat dry milk TBS containing 0.1% Tween-20, followed by incubation with horseradish peroxidase-linked anti-mouse IgG antibody (Millipore 1:5000 dilution) in TBS 0.1% Tween 20 at room temperature for 1 hour. Finally, proteins were visualized using an enhanced chemiluminescence kit (Bio-Rad,), and images were obtained using a LAS-4000 lumino-image analyzer system (Fujifilm, Tokyo, Japan).

Immunohistochemistry and Histology. Seven and fourteen days after treatment, naive and CFA-injected animals were anesthetized with chloralium hydrate (400 mg/kg i.p.) and transcardially perfused with saline followed by 4% paraformaldehyde in 0.1 M phosphate buffer. Paws and L4, L5, and L6 DRG lumbar spinal cord sections were dissected out, snap frozen in 2-methylbutane, and stored at −80°C. Tissues were fixed using a cryo-embedding media compound (optimal cutting temperature) and 40 μm (paw samples) or 20 μm sections (DRG samples) were cut and mounted onto slides. Sections were immunostained with an anti-NAAA primary antibody (1:200 dilution; Abcam UK) followed by Alexa Fluor 488 (1:1000 dilution; Life Technologies, Carlsbad, CA) secondary antibody. Images were collected with a Nikon A1 inverted confocal microscopy with a 60× 1.4 numerical aperture objective lens. A second set of paw samples were processed for histologic analysis. Sections 5 μm thick were cut with a cryostat, stained with hematoxylin and eosin (H&E), and observed with Leica DM5500 B microscope with a 40× 0.85 numerical aperture objective lens.

Lipid Extractions. Tissue FAE levels were measured as described (Astarita and Piomelli, 2009). Briefly, frozen paws were weighed ($\approx$70 mg) and homogenized in methanol (1 ml) containing

[^{2}H$_4$]-PEA and [^{2}H$_4$]-OEA as internal standards (Cayman Chemical, Ann Arbor, MI). Lipids were extracted with chloroform (2 ml) and washed with water (1 ml). After centrifugation (21,000 g, 15 minutes at 4°C), organic phases were collected and dried under nitrogen. The organic extracts were fractionated by silica gel column chromatography. PEA and OEA were eluted with chloroform/methanol (9:1, v/v). Organic phases were evaporated under nitrogen and reconstituted in 75 μl of methanol/chloroform (9:1, v/v). Liquid chromatography/mass spectrometry analyses were conducted on a Xevo TQ UPLC-MS/MS system (Waters) equipped with a reversed phase BEH C18 column (Waters), using a linear gradient of acetonitrile in water. Quantifications were performed monitoring the following MRM transitions (parent m/z ->daughter m/z, collision energy eV): OEA 326->62,20; [^{2}H$_4$]-OEA 330->66,20; PEA 300->62,20; [^{2}H$_4$]-PEA 304->66,20. Analyte peak areas were compared with a standard calibration curve (0.1 nM to 1 μM).

Pus Collection and Myeloperoxidase Activity. Pus was manually removed from dissected paws and weighed. Paws were processed to evaluate myeloperoxidase (MPO) activity. Briefly, weighed paw tissues were homogenized in phosphate buffer (1 ml, 5 mM; pH 6) and centrifuged at 21,000 g for 30 minutes at 4°C. Supernatants were discarded and pellets were washed again as described above. Pellets were suspended in a solution of 0.5% hexadecyltrimethylammonium bromide (Sigma-Aldrich, Milan, Italy) dissolved in phosphate buffer (50 mM, pH 6) and frozen at −40°C. Three freeze/thaw/sonication cycles were performed. Samples were incubated at 4°C for 10 minutes and then centrifuged at 12,500 g for 15 minutes (4°C). Supernatants were collected and 7 μl was allowed to react with 200 μl of a solution containing 167 mg/l of o-dianisidine dihydrochloride (Sigma-Aldrich) and 0.0005% hydrogen peroxide (Sigma-Aldrich) in phosphate buffer (5 mM, pH 6). Changes in absorbance were recorded at intervals of 30 seconds for 2 minutes at 460 nm using a microplate reader. One unit of MPO activity was defined as the quantity of enzyme degrading 1 μmol of hydrogen peroxide per minute at 25°C.

Activity-Based Protein Profiling. Vehicle or ARN14686 (undec-10-ynyl-N-[(3S)-2-oxoazetidin-3-yl]carbamate) (Romeo et al., 2015) was administered intravenously at the dose of 3 mg/kg to naive and CFA-injected rats 4 hours before death. Another group of rats was treated with ARN726 (3 mg/kg, i.v.) 4 hours before ARN14686. The animals were killed and their paws were snap frozen in liquid nitrogen and stored at −80°C. Lysosomal soluble protein (0.5 mg) was prepared as described above and used to perform click chemistry (Romeo et al., 2015). To label probe-bound proteins, biotin was added by click chemistry according to a protocol described in the literature (Speers and Cravatt, 2009). Briefly, the following reagents were added to 500 μg of the protein preparation (at the concentration of 1 mg/ml) at the indicated final concentration: 100 μM azide-PEG3-biotin conjugate (CLK-AZ104P4, Jena Bioscience, Jena, Germany); 1 mM tris(2-carboxyethyl)phosphine hydrochloride, 100 μM Tris[(1-benzyl-1H-1,2,3-triazol-4-yl)methyl]amine, 1 mM CuSO4.5H2O. Tris[(1-benzyl-1H-1,2,3-triazol-4-yl)methyl]amine was first dissolved in DMSO at 83.5 mM and then diluted with 4 volumes of tert-butanol. The samples were mixed, incubated for 2 hours at 25°C, and streptavidin enriched as described (Romeo et al., 2015). Proteins were extracted by two rounds of methanol/chloroform precipitation, and the protein pellet was suspended in 325 μl of SDS 2.5%. Samples were sonicated 3 × 10 seconds, heated at 65°C for 5 minutes, and sonicated again. Finally, samples were centrifuged for 4 minutes at 6500 g to remove insolubilized components, and the supernatant was stored at −20°C overnight. To enrich and purify the labeled proteome, the SDS content of the samples was diluted to 0.2% by the addition of 4 ml of PBS and streptavidin-agarose resin (40 μl of 50% slurry, product #20353, Thermo Scientific) was added for 2 hours at room temperature. The streptavidin beads were collected by centrifugation (2 minutes at 1000 g) and washed with 3 × 1 ml of: 1% SDS, 6 M urea, and PBS. The enriched proteins were eluted from the beads by adding one volume of a solution of 6 M urea, 2 M thiourea, 6 mM biotin, and 2% SDS, 15 minutes at room temperature followed by 15 minutes at

95°C (Rybak et al., 2004), and then 1× SDS-loading buffer was added. SDS-PAGE was performed and the resolved samples were transferred into nitrocellulose membranes that were blocked with 5% bovine serum albumin/PBS/0.1% Tween 20. For the detection of biotinylated samples, IRdye 680LT streptavidin (product #926-68031, LICOR Biosciences, Lincoln, NE) was added for 1 hour at room temperature. Images were acquired with a FujiFilm FLA-9000 instrument.

Data Analyses. Results are expressed as mean ± S.E.M. GraphPad Prism software (GraphPad Software, Inc., San Diego, CA) was used for statistical analysis. Data were analyzed using Student's t test or two-way analysis of variance followed by Bonferroni post hoc test for multiple comparisons. Differences between groups were considered statistically significant at values of $P < 0.05$. Significant outliers were excluded performing the Grubbs' test, considered statistically significant at values of $P < 0.05$.

Results

Effects of CFA on NAAA Levels in Paw Tissue. As expected, injection of CFA into the hindpaws of rats elicited marked local swelling and heat hypersensitivity (Fig. 1, A and B; $P < 0.001$), which lasted for the entire duration of the experiment (14 days). Concomitantly, the injected area underwent profound epidermal atrophy along with changes in dermal structure (Fig. 2, A–C). This inflammatory and tissue-damaging reaction was accompanied by a substantial increase in the levels of NAAA protein, as assessed by Western blot analyses (Fig. 1C; $P < 0.001$) and ex vivo enzyme assays (Fig. 1D; $P < 0.001$). Immunofluorescence experiments on sections
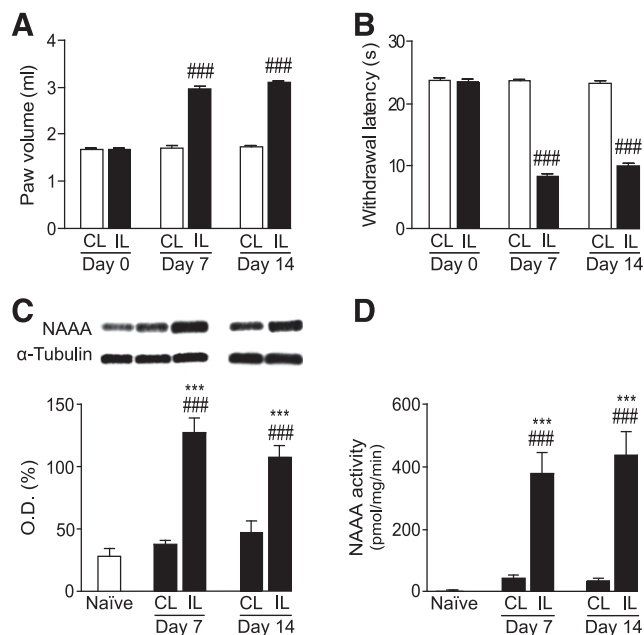

Fig. 1. CFA injection persistently increases NAAA levels in rat paws. (A and B) Effects of CFA injection on edema (A) and heat hyperalgesia (B) assessed before (day 0) and on days 7 and 14 after injection. IL, ipsilateral paws; shaded bars; CL, contralateral noninjected paws (open bars). Results are expressed as mean ± S.E.M. ### $P < 0.001$ ipsilateral versus contralateral paw ($n = 10$). (C) Representative Western blots and quantification of NAAA levels in paw tissue; alpha-tubulin was used as loading control; O.D. (%): densitometric analysis of the NAAA signal, expressed as percentage of the NAAA signal compared with alpha-tubulin signal. (D) NAAA activity in paw tissue extracts. Results are expressed as mean ± S.E.M. ***$P < 0.001$ versus control group; ###$P < 0.001$ ipsilateral versus contralateral hindpaw ($n = 5$ each).
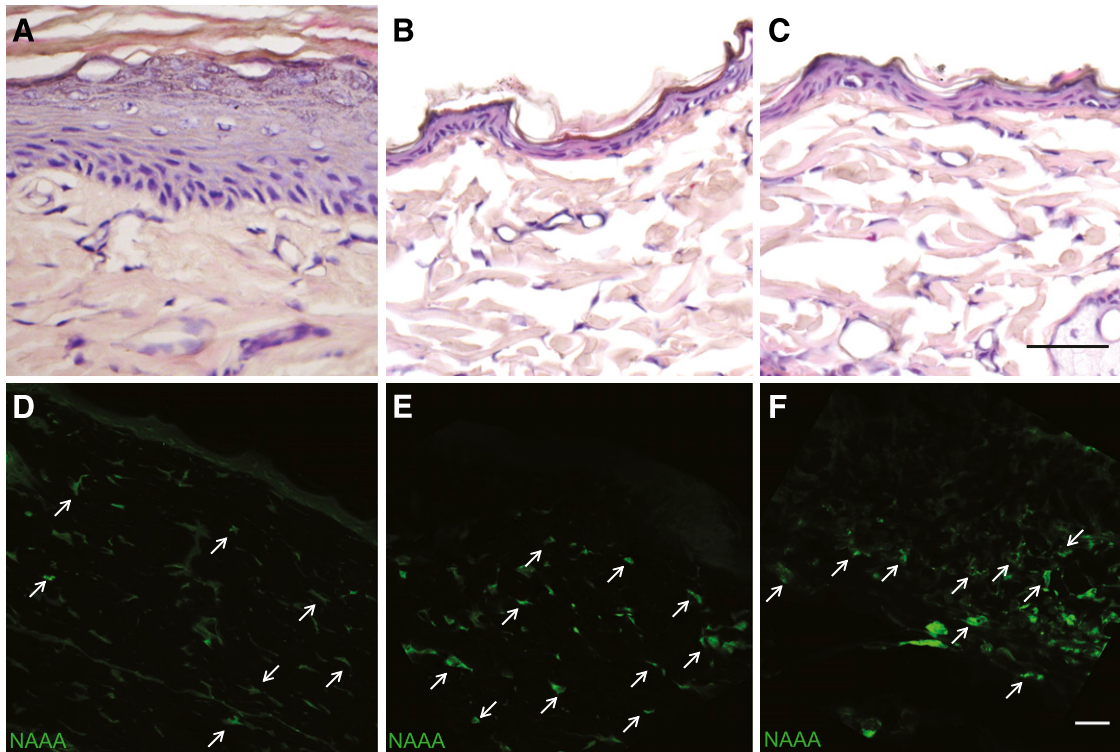
Fig. 2. CFA injection persistently increases NAAA immunoreactivity in rat paw skin. (A–C) Representative images illustrating the effects of vehicle (A) or CFA injection [7 days (B); 14 days (C)] on skin integrity, as assessed by hematoxylin-eosin (H&E) staining. (D–F) Representative images illustrating the effects of vehicle (D) or CFA injection [7 days (E); 14 days (F)] on NAAA immunofluorescence (green) in decalcified paw tissues. Scale bar: 50 μm (H&E) and 20 μm (immunofluorescence). Arrows indicate NAAA signal (n = 3 each).

of decalcified paw tissue confirmed these findings, showing that local levels of immunoreactive NAAA were markedly elevated after CFA injection (Fig. 2, D–F). Control preabsorption experiments confirming the selectivity of the NAAA antibody are illustrated in (Supplemental Fig. 1).

Effects of CFA on NAAA Levels in Dorsal Root Ganglia. Similar, albeit not identical results were obtained in dorsal root ganglia (DRG) innervating the hindpaws (L4, L5, and L6). Ex vivo enzyme assays showed that NAAA activity was higher in extracts of ipsilateral DRG from CFA-injected rats compared with DRG from naive rats or contralateral DRG (Fig. 3A; $P < 0.05$). This effect was statistically significant 7 days after injection, but disappeared by day 14 (Fig. 3A). A similar time course was observed in immunofluorescence analyses of DRG-L5. The appearance of NAAA immunoreactivity on day 7 of the experiment and its disappearance on day 14 (Fig. 3, B–D) coincided with the profile of NAAA activity changes (Fig. 3A).

Effects of ARN726 on Edema and Thermal Hyperalgesia. Systemic administration of the β-lactam-based NAAA inhibitor ARN726 (Ribeiro et al., 2015) attenuated paw edema and heat hyperalgesia produced by CFA injection in a dose-dependent manner. Single doses of the inhibitor (3, 10, and 30 mg/kg) were administered by intraperitoneal injection on days 7 and 14, 1 and 4 hours before the tests. A separate group of rats was treated with a single dose of dexamethasone (10 mg/kg, oral), a potent anti-inflammatory steroid. Edema measurements are reported in Fig. 4, A and B, as difference in paw volume before and after drug treatment. ARN726 produced a dose-dependent reduction in paw volume, which was statistically detectable 1 hour after drug administration

and was maximal at the dose of 30 mg/kg. At this dosing level, the anti-inflammatory efficacy of ARN726 was comparable to that of dexamethasone (Fig. 4, A and B). In addition, ARN726 (30 mg/kg) caused a significant attenuation in the quantity of pus and the levels of myeloperoxidase activity present in the inflamed paws (Fig. 4, C and D). The NAAA inhibitor was also able to lower heat hyperalgesia in CFA-injected paws: 1 hour after treatment, this effect was only seen at the dose of 30 mg/kg, but was evident at both 10 and 30 mg/kg 4 hours later (Fig. 5).

Effects of ARN726 on NAAA Activity and FAE Levels. Next we examined whether systemic administration of ARN726 affected NAAA activity and FAE content in the paws of rats treated with CFA. As shown in Fig. 6A, CFA injection was accompanied by an increase in NAAA in inflamed paws, as assessed by activity assays, and this effect was significantly reduced by administration of ARN726 (30 mg/kg, i.p.). ARN726 also normalized paw levels of PEA and OEA, which, as expected from previous work (Zhu et al., 2011; Sasso et al., 2013; Ribeiro et al., 2015), were lowered by treatment with CFA (Fig. 6, B and C). Similarly, the inhibitor suppressed NAAA activity in L4–L6 DRG of rats treated with CFA (Fig. 6D).

Effects of ARN726 on Catalytically Active NAAA. The catalytically competent form of NAAA is generated by N-terminal cleavage of the inactive holoenzyme (Tsuboi et al., 2007; Ribeiro et al., 2015). Cleavage occurs spontaneously in acid buffers and, for this reason, ex vivo NAAA activity assays, which are run at pH 4.5, quantify the total amount of NAAA present in a tissue rather than the quantity of active form present. To test whether CFA increases the levels of the active form of NAAA and whether ARN726 specifically interacts with such form, we used a potent and selective activity-based
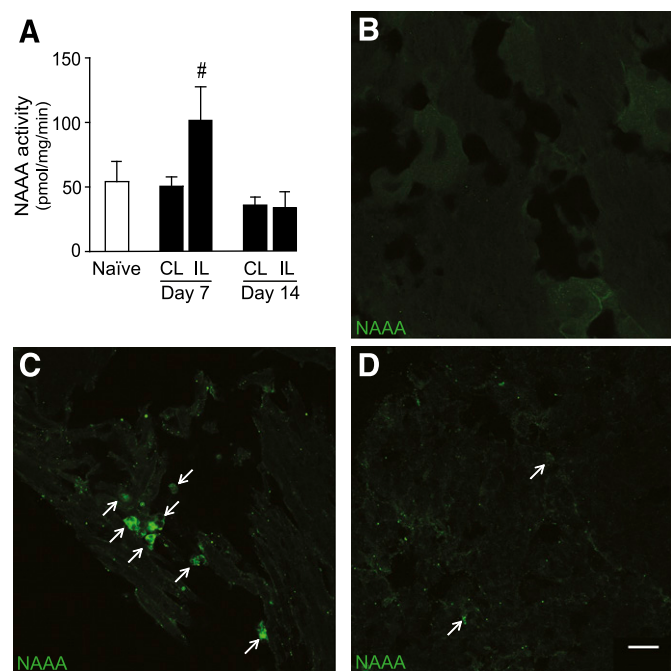
Fig. 3. CFA injection transiently increases NAAA immunoreactivity in rat DRG. (A) Effects of CFA injection on NAAA activity in DRG extracts (L4-L5-L6) from naive rats (open bar) and contralateral (CL) or ipsilateral (IL) sides (shaded bars) of CFA-injected rats, 7 and 14 days postinjection ($n = 4$ each). (B–D) Representative images of NAAA immunofluorescence in L5-DRG. Immunostaining for NAAA (green) was performed on DRG extracts from naive rats (B) or from rats that had received CFA either 7 days (C) or 14 days (D) before measurements. Scale bar: 20 μm. Arrows indicate NAAA immunofluorescence ($n = 3$). Results are expressed as mean $\pm$ S.E.M. #$P < 0.05$ ipsilateral versus contralateral DRG.

probe recently developed by our group (ARN14686, Fig. 7A) (Romeo et al., 2015). We administered vehicle or ARN14686 (3 mg/kg) by intravenous injection and profiled paw tissue for the presence of proteins that interacted with the probe. As outlined in Fig. 7A, we prepared the lysosomal protein fraction containing NAAA (Tsuboi et al., 2007) and added biotin to the chemically modified protein using click chemistry (Rostovtsev et al., 2002; Wang et al., 2003). The introduction of biotin allowed for the enrichment of probe-bound NAAA on streptavidin beads and subsequent analysis by protein blot (Fig. 7B). Inspection of the protein blots show that ARN14686 captured NAAA in the paws of CFA-treated rats (lane 4), whereas no signal was detected in the paws of naive rats (lane 2). This result indicates that inflammation is associated with NAAA activation. When rats were pretreated with ARN726 at the same intravenous dose as ARN14686 (3 mg/kg), no band corresponding to NAAA was detected (lane 5), suggesting that both compounds compete for the same site of NAAA (Romeo et al., 2015).

Discussion

Despite the availability of various classes of anti-inflammatory drugs—including corticosteroids, nonsteroidal anti-inflammatory drugs, and cytokine inhibitors (Greaves, 1976; Williams et al., 2007; Quan et al., 2008; Crofford, 2013)—nonresolving inflammatory pathologies, such as rheumatoid arthritis, remain a clinical challenge due to the partial efficacy and/or frequent side effects of existing therapies. The identification

of novel control points of inflammation is an essential step to overcome this challenge. Recent studies have suggested that the intracellular cysteine amidase NAAA may contribute to the pathogenesis of chronic inflammation by suppressing the anti-inflammatory activity of OEA and PEA, two endogenous agonists of the nuclear receptor PPAR-α (Fu et al., 2003; LoVerme et al., 2005; Piomelli and Sasso, 2014). In the present study, we investigated the contribution of NAAA to CFA-induced joint inflammation and the effects of the β-lactam-based NAAA inhibitor ARN726 in this model. We found that administration of CFA into the paw of rats causes a substantial decrement in the tissue content of PEA and OEA, as previously shown in other animal models of inflammation (Capasso et al., 2001; De Filippis et al., 2009; Solorzano et al., 2009) and in patients suffering from rheumatoid arthritis (Richardson et al., 2008). Along with changes in PEA and OEA, we found that CFA produces a marked local elevation in the catalytically active form of NAAA, which is produced by self-cleavage of the inactive holoenzyme (Tsuboi et al., 2005). Furthermore, we showed that systemic administration of ARN726 reduces NAAA activity, restores tissue PEA and OEA levels, and attenuates inflammatory symptoms in animals treated with CFA. These results provide strong evidence for a role of NAAA in CFA-induced joint inflammation and suggest that this enzyme may offer a novel target for the treatment of arthritis.

In mammalian tissues, PEA and OEA are produced through a two-step enzyme-mediated mechanism. First, an N-acyltransferase activity, which remains to be molecularly
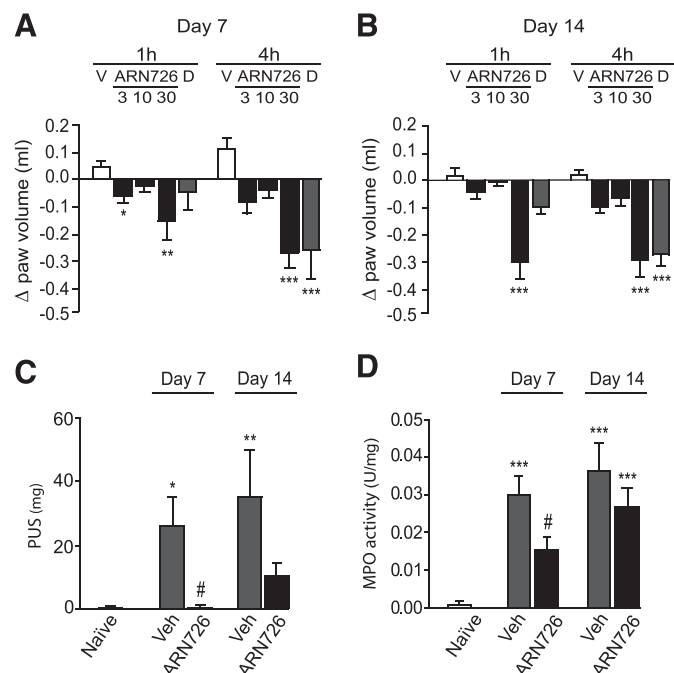

Fig. 4. The NAAA inhibitor ARN726 reduces CFA-induced inflammation. (A and B) Effects of vehicle (open bars), ARN726 (3, 10, and 30 mg/kg, i.p.; filled bars), or dexamethasone (10 mg/kg, oral; shaded bars) on paw volume, assessed 7 days (A) and 14 days (B) after CFA injection. Vehicle or drugs were injected 1 or 4 hours before tests. (C and D) Effects of vehicle (shaded bars) or ARN726 (30 mg/kg, i.p., filled bars) on pus content (C) and MPO activity (D). Edema measurements are reported as difference in paw volume before and after drug treatment. Results are expressed as mean $\pm$ S.E.M. *$P < 0.05$, **$P < 0.01$, ***$P < 0.001$ versus control group; #$P < 0.05$ ARN726 versus vehicle ($n = 5$–10).
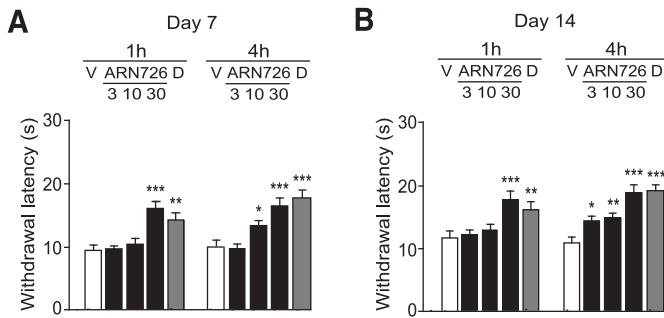
Fig. 5. The NAAA inhibitor ARN726 reduces CFA-induced heat hyperalgesia. (A and B). Effects of vehicle (open bars), ARN726 (3, 10, and 30 mg/kg, i.p.; filled bars), or dexamethasone (10 mg/kg, oral; shaded bars) on heat hyperalgesia, assessed 7 days (A) and 14 days (B) after CFA injection. Vehicle or drugs were injected 1 or 4 hours before tests. Results are expressed as mean ± S.E.M. *$P < 0.05$, **$P < 0.01$, ***$P < 0.001$ versus control group ($n = 10$).

cloned, transfers the palmitic or oleic acid chain from the sn-1 position of phosphatidylcholine to the amino group of phosphatidylethanolamine (PE). The newly formed N-acyl-PE is hydrolyzed to PEA and OEA by a selective phospholipase D, whose primary sequence and tridimensional structure have been elucidated (Okamoto et al., 2004; Wang et al., 2006; Magotti et al., 2015). Two distinct enzymes, fatty acid amide hydrolase and NAAA, are able to catalyze the hydrolysis of PEA and OEA into their constituent fatty acids and ethanolamine. Fatty acid amide hydrolase is an ubiquitous serine hydrolase that is expressed at particularly high levels in brain and liver (Desarnaud et al., 1995; Cravatt et al., 1996; McKinney and Cravatt, 2005), whereas NAAA is a cysteine amidase that is almost exclusively expressed in immune cells such as macrophages, B-lymphocytes, and, to a lesser extent, T-lymphocytes (Tsuboi et al., 2007; Ribeiro et al., 2015).

In healthy tissues, PEA and OEA are present at relatively high concentrations—in the single-digit micromolar range—which are thought to be sufficient to fully engage local PPAR-α (Piomelli and Sasso, 2014). Exposure to inflammatory stimuli causes, however, a marked drop in tissue PEA and OEA levels. For example, the PEA content in exudates from mice exposed to carrageenan is substantially lower than that of exudates obtained from naive mice (Solorzano et al., 2009). Similarly, tissue PEA levels are reduced in carrageenan-induced granuloma (De Filippis et al., 2009) and in the intestine of mice treated with croton oil (Capasso et al., 2001; Izzo et al., 2012). Experiments in the macrophage-like RAW264.7 cell line, suggest that the decrease in PEA and OEA accumulation results from transcriptional suppression of N-acyl-PE-phospholipase D expression, which is negatively controlled by activators of Toll-like receptor 4 (Zhu et al., 2011). Changes in PEA and OEA production may also contribute to the control of chronic inflammation in humans: this possibility is supported by studies showing that synovial levels of these substances are dramatically reduced in subjects with rheumatoid arthritis and osteoarthritis, relative to healthy controls (Richardson et al., 2008).

The finding that NAAA is highly expressed in macrophages suggests that this enzyme may contribute to the regulation of the innate immune response. Pharmacological studies support this idea. Two main classes of potent NAAA inhibitors have been characterized so far (for review, see Pontis et al., 2015). The first is represented by β-lactone derivatives such as
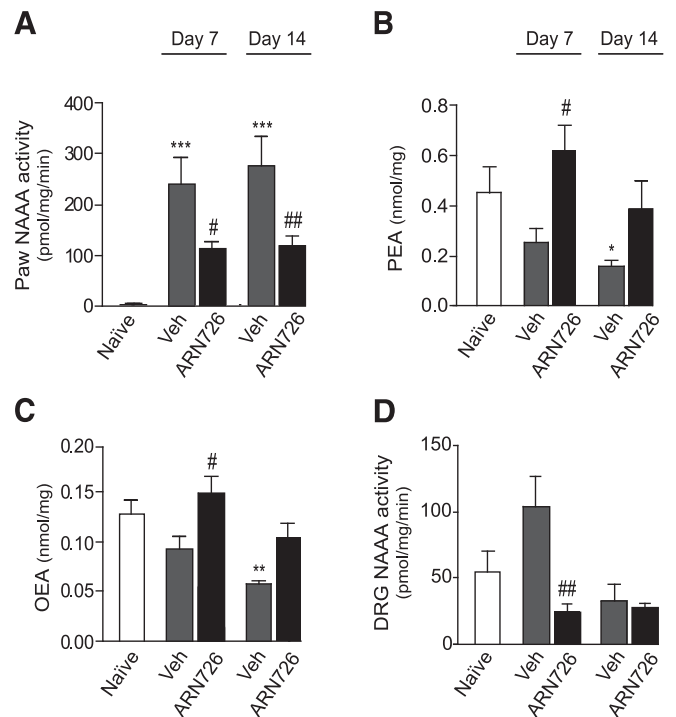

Fig. 6. The NAAA inhibitor ARN726 lowers NAAA activity and normalizes PEA and OEA levels in CFA-injected paws. (A–C) Effects of vehicle (shaded bars) and ARN726 (30 mg/kg, i.p.; closed bars) on NAAA activity (A), PEA levels (B), and OEA levels (C) in CFA-injected rat paws. Data for naive rat paws are also shown (open bars). (D) Effects of vehicle (shaded bars) and ARN726 (30 mg/kg, i.p.; closed bars) on NAAA activity in DRG extracts (L4-L5-L6) from naive rats (open bar) or CFA-injected rats. Results are expressed as mean ± S.E.M. *$P < 0.05$, **$P < 0.01$, ***$P < 0.001$ versus control group; #$P < 0.05$, ##$P < 0.01$ ARN726 versus vehicle ($n = 5$).

N-[(3S)-2-oxo-3-oxetanyl]-3-phenylpropanamide [(S)-OOPP], which inhibits NAAA activity in vitro with an IC_{50} of 420 nM (Solorzano et al., 2009). When tested on RAW264.7 cells stimulated with lipopolysaccharide (LPS), (S)-OOPP lowered NAAA activity and normalized PEA levels in the presence of LPS (Solorzano et al., 2009). Moreover, in vitro studies demonstrated that (S)-OOPP reduces carrageenan-induced leukocyte migration (Solorzano et al., 2009). Importantly, (S)-OOPP did not decrease inflammatory responses in PPAR-α deficient mice, whereas PPAR-α agonists mimicked its anti-inflammatory effects, providing evidence that NAAA inhibition restores PEA and OEA signaling at PPAR-α during inflammation and blocks tissue reactions to inflammatory stimuli. Subsequent investigations led to the identification of another β-lactone derivative, (2S,3R)-2-methyl-4-oxo-3-oxetanylcarbamic acid 5-phenylpentyl ester (ARN077), which inhibits NAAA with high potency ($IC_{50} = 50$ nM on rat NAAA and 7 nM on human NAAA) and selectivity (Ponzano et al., 2013; Sasso et al., 2013) through a covalent mechanism (Armirotti et al., 2012). However, because of its intrinsic metabolic instability, ARN077 is most effective when directly applied to an inflamed area of tissue (Sasso et al., 2013).

A second, more recent class of NAAA inhibitors comprises β-lactam derivatives that partially overcome the metabolic instability issues seen with β-lactone compounds (Ribeiro et al., 2015). The prototype member of this class, ARN726, potently inhibits NAAA activity both in vitro ($IC_{50} = 63$ nM on
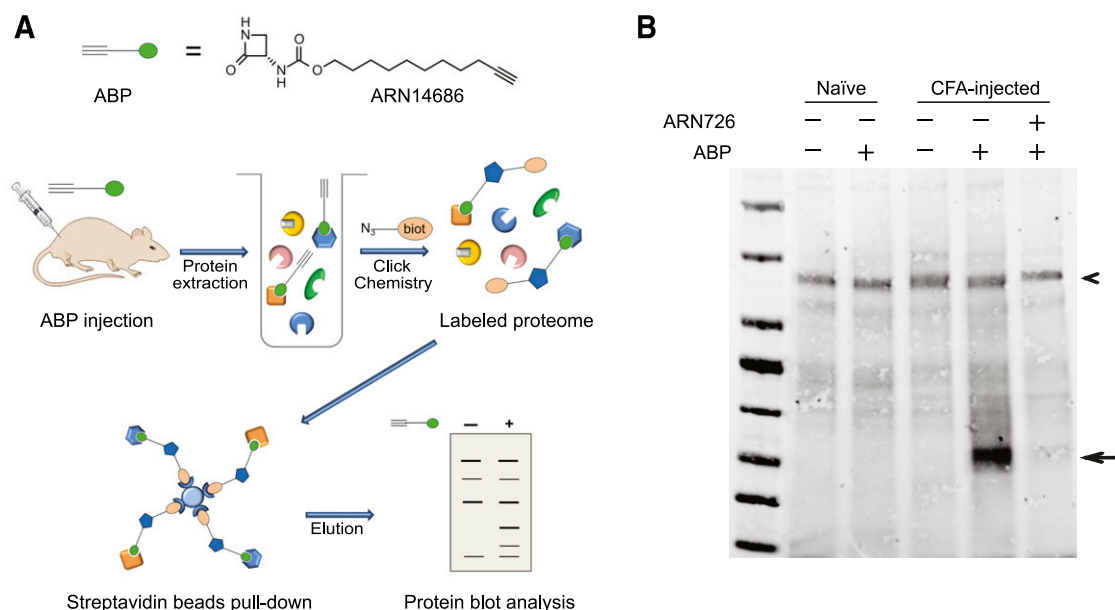
Fig. 7. CFA injection causes a persistent activation of NAAA in rat paws. (A) Scheme illustrating the procedure used: chemical structure of NAAA-specific activity-based probe, ARN14686, and main steps of the protocol are reported. (B) Protein blot analysis of streptavidin-enriched proteins from naïve rats (lanes 1, 2) or CFA-injected rats 7 days after injection (lanes 3–5). Rats received intravenous injections of vehicle or ARN14686 (3 mg/kg). Another set of CFA-injected rats was pretreated with ARN726 (3 mg/kg, lane 5). The arrow indicates the NAAA band; the arrowhead indicates a biotin-containing band of around 90 kDa, showing that a similar amount of protein was loaded in each lane.

rat NAAA and 27 nM on human NAAA) and in vivo and suppresses lung inflammation in mice via a mechanism that requires PPAR-α activation (Ribeiro et al., 2015). Additionally, ARN726 suppresses lung inflammation in mice, via a mechanism that requires PPAR-α activation, and blunts endotoxin-induced responses in human macrophages (Ribeiro et al., 2015). The present findings provide additional support to the possibility that inhibition of intracellular NAAA activity results in anti-inflammatory effects, which are comparable in efficacy to those exerted by the synthetic corticosteroid dexamethasone.

Our results also suggest that NAAA expression may play a direct role in the development of an inflammatory reaction. Using a combination of Western blot analysis and in vivo activity-based profiling, we have shown that the catalytically active form of NAAA accumulates at foci of inflammation (e.g., sites of CFA injection) as well as in the DRG innervating those sites. NAAA accumulation might result from increased expression by resident macrophages and/or by infiltration of blood-borne monocytes, B-lymphocytes, or T-lymphocytes, which all express the enzyme at various levels (Ribeiro et al., 2015). Notably, we found that CFA-induced inflammation is accompanied by a transient (on day 7, but not 14) increment in NAAA activity in lumbar DRG, which is tempered by NAAA inhibition. Recent work has shown that NAAA is expressed in the DRG, where it may contribute to the control of nociceptive processing through regulation of PEA and OEA signaling at PPAR-α (Khasabova et al., 2012). These data suggest that the increase in NAAA levels observed in the present experiments may be due to enhanced expression by DRG neurons or other resident cells. However, migration of macrophages to the DRG has been observed in the CFA model (Inglis et al., 2005) as well as in other animal models of arthritis (Segond von Banchet et al., 2009) and nerve injury (Zimmermann, 2001), and it is strongly related to the development of mechanical hyperalgesia (Inglis et al., 2005). It is also possible, therefore, that NAAA is transported by monocytes infiltrating into the DRG. Irrespective of its origin, our results show that the increase in NAAA expression is accompanied by a decrease in the levels of PEA and OEA, which might contribute to the induction of inflammation by CFA.

In summary, our results suggest the involvement of the catalytically active form of NAAA in the inflammatory process elicited by CFA injection. ARN726 is able to alleviate symptoms associated with arthritis induction selectively inhibiting NAAA activity not only in paw tissues, where PEA and OEA levels are restored, but also in lumbar DRG, where an initial increment in NAAA level was detected. These findings indicate that NAAA inhibition might represent a useful approach to treat pain and inflammation in arthritic diseases.

References

Armirotti A, Romeo E, Ponzano S, Mengatto L, Dionisi M, Karacsonyi C, Bertozzi F, Garau G, Tarozzo G, and Reggiani A, et al. (2012) β-Lactones inhibit N-acylethanolamine acid amidase by S-acylation of the catalytic N-terminal cysteine. *ACS Med Chem Lett* **3**:422–426.

Astarita G and Piomelli D (2009) Lipidomic analysis of endocannabinoid metabolism in biological samples. *J Chromatogr B Analyt Technol Biomed Life Sci* **877**: 2755–2767.

Capasso R, Izzo AA, Fezza F, Pinto A, Capasso F, Mascolo N, and Di Marzo V (2001) Inhibitory effect of palmitoylethanolamide on gastrointestinal motility in mice. *Br J Pharmacol* **134**:945–950.

Cravatt BF, Giang DK, Mayfield SP, Boger DL, Lerner RA, and Gilula NB (1996) Molecular characterization of an enzyme that degrades neuromodulatory fatty-acid amides. *Nature* **384**:83–87.

Crofford LJ (2013) Use of NSAIDs in treating patients with arthritis. *Arthritis Res Ther* **15** (Suppl 3):2–10.

De Filippis D, D'Amico A, Cinelli MP, Esposito G, Di Marzo V, and Iuvone T (2009) Adelmidrol, a palmitoylethanolamide analogue, reduces chronic inflammation in a carrageenin-granuloma model in rats. *J Cell Mol Med* **13**:1086–1095.

Desarnaud F, Cadas H, and Piomelli D (1995) Anandamide amidohydrolase activity in rat brain microsomes. Identification and partial characterization. *J Biol Chem* **270**:6030–6035.

Fu J, Gaetani S, Oveisi F, Lo Verme J, Serrano A, Rodríguez De Fonseca F, Rosengarth A, Luecke H, Di Giacomo B, and Tarzia G, et al. (2003) Oleylethanolamide regulates feeding and body weight through activation of the nuclear receptor PPAR-alpha. *Nature* **425**:90–93.

Greaves MW (1976) Anti-inflammatory action of corticosteroids. *Postgrad Med J* **52**:631–633.

Hargreaves K, Dubner R, Brown F, Flores C, and Joris J (1988) A new and sensitive method for measuring thermal nociception in cutaneous hyperalgesia. *Pain* **32**:77–88.

Inglis JJ, Nissim A, Lees DM, Hunt SP, Chernajovsky Y, and Kidd BL (2005) The differential contribution of tumour necrosis factor to thermal and mechanical hyperalgesia during chronic inflammation. *Arthritis Res Ther* **7**:R807–R816.

Izzo AA, Capasso R, Aviello G, Borrelli F, Romano B, Piscitelli F, Gallo L, Capasso F, Orlando P, and Di Marzo V (2012) Inhibitory effect of cannabichromene, a major non-psychotropic cannabinoid extracted from Cannabis sativa, on inflammation-induced hypermotility in mice. *Br J Pharmacol* **166**:1444–1460.

Khasabova IA, Xiong Y, Coicou LG, Piomelli D, and Seybold V (2012) Peroxisome proliferator-activated receptor α mediates acute effects of palmitoylethanolamide on sensory neurons. *J Neurosci* **32**:12735–12743.

Laskin DL, Sunil VR, Gardner CR, and Laskin JD (2011) Macrophages and tissue injury: agents of defense or destruction? *Annu Rev Pharmacol Toxicol* **51**:267–288.

LoVerme J, La Rana G, Russo R, Calignano A, and Piomelli D (2005) The search for the palmitoylethanolamide receptor. *Life Sci* **77**:1685–1698.

Magotti P, Bauer I, Igarashi M, Babagoli M, Marotta R, Piomelli D, and Garau G (2015) Structure of human N-acylphosphatidylethanolamine-hydrolyzing phospholipase D: regulation of fatty acid ethanolamine biosynthesis by bile acids. *Structure* **23**:598–604.

McKinney MK and Cravatt BF (2005) Structure and function of fatty acid amide hydrolase. *Annu Rev Biochem* **74**:411–432.

Okamoto Y, Morishita J, Tsuboi K, Tonai T, and Ueda N (2004) Molecular characterization of a phospholipase D generating anandamide and its congeners. *J Biol Chem* **279**:5298–5305.

Piomelli D and Sasso O (2014) Peripheral gating of pain signals by endogenous lipid mediators. *Nat Neurosci* **17**:164–174.

Pontis S, Ribeiro A, Sasso O, and Piomelli D (2015) Macrophage-derived lipid agonists of PPAR-α as intrinsic controllers of inflammation. *Crit Rev Biochem Mol Biol*, in press.

Ponzano S, Bertozzi F, Mengatto L, Dionisi M, Armirotti A, Romeo E, Berteotti A, Fiorelli C, Tarozzo G, and Reggiani A, et al. (2013) Synthesis and structure-activity relationship (SAR) of 2-methyl-4-oxo-3-oxetanylcarbamic acid esters, a class of potent N-acylethanolamine acid amidase (NAAA) inhibitors. *J Med Chem* **56**:6917–6934.

Quan LD, Thiele GM, Tian J, and Wang D (2008) The development of novel therapies for rheumatoid arthritis. *Expert Opin Ther Pat* **18**:723–738.

Ribeiro A, Pontis S, Mengatto L, Armirotti A, Chiurchiù V, Capurro V, Fiasella A, Nuzzi A, Romeo E, and Moreno-Sanz G, et al. (2015) A potent systemically active N-acylethanolamine acid amidase inhibitor that suppresses inflammation and human macrophage activation. *ACS Chem Biol* **10**:1838–1846.

Richardson D, Pearson RG, Kurian N, Latif ML, Garle MJ, Barrett DA, Kendall DA, Scammell BE, Reeve AJ, and Chapman V (2008) Characterisation of the cannabinoid receptor system in synovial tissue and fluid in patients with osteoarthritis and rheumatoid arthritis. *Arthritis Res Ther* **10**(2):R431–14

Romeo E, Ponzano S, Armirotti A, Summa M, Bertozzi F, Garau G, Bandiera T, and Piomelli D (2015) Activity-Based Probe for N-Acylethanolamine Acid Amidase. *ACS Chem Biol* **10**:2057–2064.

Rostovtsev VV, Green LG, Fokin VV, and Sharpless KB (2002) A stepwise huisgen cycloaddition process: copper(I)-catalyzed regioselective "ligation" of azides and terminal alkynes. *Angew Chem Int Ed Engl* **41**:2596–2599.

Rybak JN, Scheurer SB, Neri D, and Elia G (2004) Purification of biotinylated proteins on streptavidin resin: a protocol for quantitative elution. *Proteomics* **4**:2296–2299.

Sasso O, Bertorelli R, Bandiera T, Scarpelli R, Colombano G, Armirotti A, Moreno-Sanz G, Reggiani A, and Piomelli D (2012) Peripheral FAAH inhibition causes profound antinociception and protects against indomethacin-induced gastric lesions. *Pharmacol Res* **65**:553–563.

Sasso O, Moreno-Sanz G, Martucci C, Realini N, Dionisi M, Mengatto L, Duranti A, Tarozzo G, Tarzia G, and Mor M, et al. (2013) Antinociceptive effects of the N-acylethanolamine acid amidase inhibitor ARN077 in rodent pain models. *Pain* **154**:350–360.

Segond von Banchet G, Boettger MK, Fischer N, Gajda M, Bräuer R, and Schaible HG (2009) Experimental arthritis causes tumor necrosis factor-alpha-dependent infiltration of macrophages into rat dorsal root ganglia which correlates with pain-related behavior. *Pain* **145**:151–159.

Solorzano C, Zhu C, Battista N, Astarita G, Lodola A, Rivara S, Mor M, Russo R, Maccarrone M, and Antonietti F, et al. (2009) Selective N-acylethanolamine-hydrolyzing acid amidase inhibition reveals a key role for endogenous palmitoylethanolamide in inflammation. *Proc Natl Acad Sci USA* **106**:20966–20971.

Speers AE and Cravatt BF (2009) Activity-Based Protein Profiling (ABPP) and Click Chemistry (CC)-ABPP by MudPIT Mass Spectrometry. *Curr Protoc Chem Biol* **1**:29–41.

Tsuboi K, Sun YX, Okamoto Y, Araki N, Tonai T, and Ueda N (2005) Molecular characterization of N-acylethanolamine-hydrolyzing acid amidase, a novel member of the choloylglycine hydrolase family with structural and functional similarity to acid ceramidase. *J Biol Chem* **280**:11082–11092.

Tsuboi K, Zhao LY, Okamoto Y, Araki N, Ueno M, Sakamoto H, and Ueda N (2007) Predominant expression of lysosomal N-acylethanolamine-hydrolyzing acid amidase in macrophages revealed by immunochemical studies. *Biochim Biophys Acta* **1771**:623–632.

Wang J, Okamoto Y, Morishita J, Tsuboi K, Miyatake A, and Ueda N (2006) Functional analysis of the purified anandamide-generating phospholipase D as a member of the metallo-beta-lactamase family. *J Biol Chem* **281**:12325–12335.

Wang Q, Chan TR, Hilgraf R, Fokin VV, Sharpless KB, and Finn MG (2003) Bioconjugation by copper(I)-catalyzed azide-alkyne [3 + 2] cycloaddition. *J Am Chem Soc* **125**:3192–3193.

Williams RO, Paleolog E, and Feldmann M (2007) Cytokine inhibitors in rheumatoid arthritis and other autoimmune diseases. *Curr Opin Pharmacol* **7**:412–417.

Zhu C, Solorzano C, Sahar S, Realini N, Fung E, Sassone-Corsi P, and Piomelli D (2011) Proinflammatory stimuli control N-acylphosphatidylethanolamine-specific phospholipase D expression in macrophages. *Mol Pharmacol* **79**:786–792.

Zimmermann M (2001) Pathobiology of neuropathic pain. *Eur J Pharmacol* **429**:23–37.

Address correspondence to: Daniele Piomelli, Department of Anatomy and Neurobiology, University of California, Irvine, CA 92697-4621. E-mail: piomelli@uci.edu